AF Relaying for FBMC Signals

David Gregoratti and Xavier Mestre
Centre Tecnològic de Telecomunicacions de Catalunya (CTTC)
Parc Mediterrani de la Tecnologia - 08860 - Castelldefels - Barcelona (Spain)
email:{david.gregoratti, xavier.mestre}@cttc.es

***Abstract*—An AF relay splits an FBMC transmission link into a two-hop channel. The receiver implements a parallel multistage FBMC demodulator/equalizer that is suitable for fading channels whose frequency response cannot be considered flat over the subcarriers. The signal quality at the output of such a receiver is characterized in terms of signal-to-noise-plus-distortion ratio (SNDR), that takes into account the residual interference after equalization and the effect of the noise collected on both hops. The SNDR is then used to estimate the spectral efficiency of the link. The comparison with the direct link shows that the AF-relay scheme offers some gain, especially in lossy environments with high path-loss exponent.**

I. Introduction

Lately, a lot of effort has been driven towards the analysis and specification of Public Protection and Disaster Relief (PPDR) communications systems [1]. These networks are based on Private Mobile Radio (PMR) systems and are thought to be easily and quickly deployed to offer communication capabilities (both in terms of voice and data) in areas affected by calamity, where local telecommunications infrastructures can be damaged or insufficient.

While today's PPDR systems are based on voice/low data-rate standards like TETRA, the motivation behind a considerable number of research projects (like, e.g., the EU-funded projects [2]–[4]) is to find solutions that offer high throughput for applications such as video conferencing or on-line access to databases. Apart from hoping for competent authorities to assign a larger bandwidth to PPDR systems, new approaches are investigated that exploit the available resources more efficiently. In this perspective, filter bank multicarrier (FBMC) modulations show promising characteristics since they are robust to frequency-selective fading channels and allow a flexible occupation of the spectrum by a proper allocation of the subcarriers to the users. Moreover, as compared to classical orthogonal frequency-division multiplexing (OFDM), FBMC achieves a better exploitation of the bandwidth, since no cyclic prefix is needed and since subcarrier bands are better contained.

Another artifice that may find application in PPDR systems to improve coverage and/or signal quality is the introduction of amplify-and-forward (AF) relays. An AF relay [5] is a simple device that retransmits the received signal with no processing other than a simple amplification (a multiplication by a constant factor). It is then cheap and transparent to the characteristics of the hosting communications system. These characteristics are certainly welcome in disaster areas, since relays may be difficult to recuperate and may be required to help different services.

In this paper we combine the two strategies, namely FBMC and AF relaying, and characterize the resulting system in terms of spectral efficiency. Note that the main drawback of AF relaying is the fact that, together with the data signal, the relay amplifies and forwards also the noise collected while listening to the uplink (i.e., source–relay) channel. Thus, we will need to describe the contribution of this noise at the output of the FBMC demodulator/equalizer. In order to be as general as possible, we assume that we are dealing with highly frequency selective channels and that a simple equalizer with a single tap per subcarrier is not optimal. More specifically, we consider the parallel multistage equalizer proposed in [6], and we extend the associated concept of signal-to-noise-plus-distortion ratio (SNDR) to the relay case. Finally, by plugging the SNDR into the Shannon's spectral efficiency formula, we numerically evaluate the performance of the AF scheme and we compare it to the direct link and to the decode-and-forward (DF) relay case.

II. Signal Model and Analysis

A. Point-to-Point Case

To start with, let us summarize the main results of [6]. Indeed, the results on the FBMC/AF relay channel are much easier to explain and understand having at hand those for the point-to-point link.

Consider a single-antenna, M-subcarrier FBMC/OQAM system (with M a power of 2). Then, the output of the FBMC modulator con be written as

$$\mathbf{x} = \operatorname{vec}(\begin{bmatrix}\mathbf{X}_1 & \mathbf{0}\end{bmatrix} + \begin{bmatrix}\mathbf{0} & \mathbf{X}_2\end{bmatrix}),$$

where $\operatorname{vec}(\cdot)$ piles the columns of a matrix and

$$\mathbf{X} = \begin{bmatrix}\mathbf{X}_1 \\ \mathbf{X}_2\end{bmatrix} = \sqrt{2}(\mathbf{F}_M\boldsymbol{\Phi}^*(\mathbf{B}\otimes[1,0]+j\mathbf{C}\otimes[0,1])\circledast(\mathbf{P}\otimes[1,0]))$$

is the matrix collecting the modulated symbols. In the last equation we have also introduced the $M\times M$ Fourier matrix $[\mathbf{F}_M]_{1\le m,n\le M} = M^{-\frac{1}{2}}\exp[j\frac{2\pi}{M}(m-1)(n-1)]$, the diagonal weight matrix $\boldsymbol{\Phi} = \operatorname{diag}_{m=1,\dots,M}\{\exp[-j\pi\frac{M+2}{2M}(m-1)]\}$

This work was partially supported by the European Commission under project 7FP ICT 318362 and by the Spanish Ministry of Science and Education under grant TEC2011-29006-C03-01.

978-1-4799-5280-9/14/$31.00©2014 IEEE

and the $M \times \kappa$ matrix

$$\mathbf{P} = \begin{bmatrix} \mathbf{P}_1 \\ \mathbf{P}_2 \end{bmatrix} = \begin{bmatrix} p_N[1] & \cdots & p_N[M(\kappa-1)+1] \\ \vdots & \ddots & \vdots \\ p_n[M] & \cdots & p_N[M\kappa] \end{bmatrix}, \quad (1)$$

where $p_N[n], n = 1, \dots, N$, is the real-valued prototype pulse of length $N = M\kappa$ and $\kappa \in \mathbb{N}$ is the overlapping factor. Moreover, the operators $\otimes$ and $\circledast$ stand for the Kronecker product and the row-wise matrix convolution, respectively. Finally, the $M \times N_s$ matrix $\mathbf{A} = \mathbf{B} + j\mathbf{C}$ gathers the N_s complex multiband symbols to transmit. The elements of $\mathbf{B}$ and $\mathbf{C}$ are modeled as i.i.d. real random variables with zero mean and variance $P_{tx}/2$.

Assume now that the signal $\mathbf{x}$ is sent through a frequency-selective, time-invariant fading channel $h_0[l], l = 1, \dots, L_0$, to a K-stage FBMC demodulator/equalizer with prototype pulse $q_N[n], n = 1, \dots, N$, like the one presented in [6]. Also, the signal is deteriorated by an additive circularly symmetric white Gaussian noise process with zero mean and variance σ_d^2. Then, [6] shows that the quality of the received signal at subcarrier m can be represented by the so called signal-to-noise-plus-distortion ratio (SNDR) as long as the number of subcarriers M is large enough and the prototype pulses (i.e. $p_N[n]$ and $q_N[n]$) satisfy some continuity constraints and the following reconstruction conditions:

$$\begin{aligned} &(\mathbf{I}_2 \otimes (\mathbf{I}_{M/2} + \mathbf{J}_{M/2}))\mathcal{R}(p_n, q_N) \\ &\qquad = \begin{bmatrix} \mathbf{0}_{M\times(\kappa-1)} & \mathbf{1}_M & \mathbf{0}_{M\times(\kappa-1)} \end{bmatrix}, \\ &(\mathbf{I}_2 \otimes (\mathbf{I}_{M/2} - \mathbf{J}_{M/2}))\mathcal{S}(p_n, q_N) = \mathbf{0}_{M\times(2\kappa-1)}. \end{aligned}$$

In the last equation we have introduced the matrices

$$\mathcal{R}(p_n, q_N) = \begin{bmatrix} \mathbf{P}_1 \circledast \mathbf{J}_{M/2}\mathbf{Q}_2 \\ \mathbf{P}_2 \circledast \mathbf{J}_{M/2}\mathbf{Q}_1 \end{bmatrix}, \quad (2a)$$

$$\mathcal{S}(p_n, q_N) = \begin{bmatrix} \mathbf{P}_2 \circledast \mathbf{J}_{M/2}\mathbf{Q}_2 \\ \mathbf{P}_1 \circledast \mathbf{J}_{M/2}\mathbf{Q}_1 \end{bmatrix}, \quad (2b)$$

where $\mathbf{Q}$ is build from $q_N[n]$ as $\mathbf{P}$ from $p_N[n]$ in (1) and where $\mathbf{1}_M$, $\mathbf{J}_X$ and $\mathbf{0}_{M\times X}$ are the column vector of M ones, the $X \times X$ anti-diagonal matrix and the $M \times X$ matrix filled with zeros, respectively.

More specifically, at the output of a K-stage demodulator/equalizer[1], the SNDR for subcarrier m is given by

$$SNDR_{K,0}(m) = \frac{P_{tx}}{P_{e,0}^{(K)}(m) + P_{w,0}^{(K)}(m)}, \quad (3)$$

where the residual interference power $P_{e,0}^{(K)}(m)$ (due to a nonperfect equalizer) and the noise power $P_{w,0}^{(K)}(m)$ are given by

$$\begin{aligned} P_{e,0}^{(K)}(m) = \frac{2P_{tx}}{M^{2K+1}} \Bigg(&\mathrm{Re}^2 \left\{\mathbf{K}_K\right\}_m \mathrm{tr}\Big[\mathcal{X}_{RR}^{(K)}\mathbf{U}^+ + \mathcal{X}_{SS}^{(K)}\mathbf{U}^-\Big] \\ &+ \mathrm{Im}^2 \left\{\mathbf{K}_K\right\}_m \mathrm{tr}\Big[\mathcal{X}_{RR}^{(K)}\mathbf{U}^- + \mathcal{X}_{SS}^{(K)}\mathbf{U}^+\Big] \Bigg), \end{aligned} \quad (4)$$

and

$$P_{w,0}^{(K)}(m) = \frac{2\sigma^2}{M} \sum_{l=0}^{K-1} \sum_{r=0}^{K-1} \frac{\mathrm{Re}\left\{\mathbf{K}_l\mathbf{K}_r^*\right\}_m}{M^{l+r}\left|\left\{\mathbf{\Lambda}_{H^{(0)}}\right\}_m\right|^2} \sum_{n=1}^{M} \left\{\mathbf{r}_{l,r}\right\}_n, \quad (5)$$

respectively. We had to introduce the following quantities:

- $q_N^{(l)}, l = 1, \dots, K$, is the l-th derivative of the prototype pulse q_N;
- $\mathcal{X}_{RR}^{(K)} = \mathcal{R}(p_N, q_N^{(K)})\mathcal{R}^T(p_N, q_N^{(K)})$ and $\mathcal{X}_{SS}^{(K)} = \mathcal{S}(p_N, q_N^{(K)})\mathcal{S}^T(p_N, q_N^{(K)})$, with $\mathcal{R}(\cdot,\cdot)$ and $\mathcal{S}(\cdot,\cdot)$ defined as in (2);
- the diagonal matrices $\mathbf{\Lambda}_{H^{(r)}}, r = 0, \dots, K$ are built from the channel impulse response $h_0[l]$ according to $\left\{\mathbf{\Lambda}_{H^{(r)}}\right\}_m = \sum_{l=1}^{L_0} (-j(l-1))^r h_0[l] \exp[-j\frac{2\pi}{M}(m-1)(l-1)]$;
- the diagonal matrices $\mathbf{K}_l, l = 1, \dots, K$, are built recursively as $\mathbf{K}_l = -\mathbf{\Lambda}_{H^{(0)}}^{-1} \sum_{m=0}^{l-1} \frac{(-j)^{l-m}}{(l-m)!} \mathbf{\Lambda}_{H^{(l-m)}}\mathbf{K}_m$, starting from $\mathbf{K}_0 = \mathbf{I}_M$;
- the matrices $\mathbf{U}^\pm = \mathbf{I}_2 \otimes (\mathbf{I}_{M/2} \pm \mathbf{J}_{M/2})$ and
- the vector $\mathbf{r}_{l,r} = \left\{\mathcal{R}\left(\tilde{q}_N^{(l)}, q_N^{(r)}\right)\right\}_{:,\kappa}$, that is the κ-th column of $\mathcal{R}\left(\tilde{q}_N^{(l)}, q_N^{(r)}\right)$, with $\tilde{q}_N^{(l)}[n] = q_N^{(l)}[N-n+1]$.

B. Relay Case

Assume now that the signal $\mathbf{x}$ is not received by the destination directly, as explained above, but it rather takes advantage of an AF relay to improve, hopefully, coverage and/or signal quality. Note that, in this case, we are simply interested in the two-hop link source–relay–destination and that we will assume that the destination does not receive any signal directly from the source. For this reason, there will be no gain due to higher diversity.

Let $h_u[l], l = 1, \dots, L_u$, and $h_d[l], l = 1, \dots, L_d$, be the source–relay (uplink) and relay–destination (downlink) channels, respectively. Also, let $\sqrt{A}, A \in \mathbb{R}^+$, the amplification factor at the relay, meaning that the relay forwards the signal of the uplink channel into the downlink channel after multiplying it by $\sqrt{A}$. It is not difficult to see that the relay has a two-fold effect on the signal model: first, the equivalent channel seen by the data signal from the source to the destination is $h_{eq}[l] = \sqrt{A}(h_u * h_d)[l], l = 1, \dots, L_{eq}$, with $L_{eq} = L_u + L_d - 1$. Second, apart from the noise collected at the destination, the relay also amplifies and forwards the noise of the uplink channel. In what follows, this latter noise is modeled as an additive circularly symmetric white Gaussian noise with zero mean and variance σ_u^2. Combining the point-to-point model of the previous section with these comments, the following result is quite intuitive.

Proposition 1: Consider the FBMC/AF relay channel described above, and recall that we are making assumptions (**As1**)–(**As4**) of [6]. Then, at the output of the parallel K-stage FBMC demodulator/equalizer, the quality of the signal at the m-th subcarrier can be represented by

$$SNDR_{K,\mathrm{AF}}(m) = \frac{P_{tx}}{P_{e,\mathrm{AF}}^{(K)}(m) + P_{w,d}^{(K)}(m) + P_{w,u}^{(K)}(m)}. \quad (6)$$

[1]For $K = 1$, the equalizer reduces to the classical single-tap per subcarrier equalizer. For larger K, see [6] for further details.

The first and second term of the denominator can be computed as in (4) and (5), respectively, after substituting the direct channel $h_0[l]$ with the equivalent channel $h_{eq}[l]$ (recall that the matrices $\mathbf{K}_l$ and $\mathbf{\Lambda}_{H^{(r)}}$ are also functions of the channel impulse response and, thus, must be computed with respect to $h_{eq}[l]$). The last term, instead, corresponds to the power of the noise that the relay collects in the uplink and forwards to the destination. It is given by:

$$P_{w,u}^{(K)}(m) = \frac{2A\sigma_u^2}{M} \sum_{l,r=0}^{K-1} \sum_{s,t=1}^{L_d} \frac{\sum_{n=1}^{M} \{\mathbf{r}_{l,r}^{s,t}\}_n}{M^{l+r} |\{\mathbf{\Lambda}_{H^{(0)}}\}_m|^2} \times \mathrm{Re}\left\{h_d[s]h_d^*[t]\mathbf{K}_l\mathbf{\Theta}_M^{s-1}(\mathbf{K}_r\mathbf{\Theta}_M^{t-1})^*\right\}_m, \quad (7)$$

where we have introduced the diagonal matrix $\mathbf{\Theta}_M = \mathrm{diag}_{m=1,\dots,M}\{\exp[-j\frac{2\pi}{M}(m-1)]\}$ and denoted $\mathbf{r}_{l,r}^{s,t}$ the $(\kappa+1)$-th column of $\mathcal{R}\left(\tilde{q}_N^{(l)}(s), q_N^{(r)}(t)\right)$, with $q_N(s)[n] = q_N[n-s+1]$ a delayed version of $q_N[n]$ and, as before, $q_N^{(l)}(s)$ its l-th derivative, whereas $\tilde{q}_N^{(l)}(s)$ indicates that time has been reversed.

Proof: As mentioned before, if we could neglect the noise introduced by the relay (i.e., $\sigma_u^2 = 0$), the system would behave exactly as the point-to-point case introduced in the previous section. The only difference would be that the data signal now sees the equivalent channel $h_{eq}[l] = \sqrt{A}(h_u * h_d)[l]$ instead of the direct channel $h_0[l]$. Thus, the interference power $P_{e,\mathrm{AF}}^{(K)}(m)$ and the downlink noise power $P_{w,d}^{(K)}(m)$ can be computed as in (4) and (5), respectively, with the appropriate channel corrections. Then, we only need to prove (7).

Similarly to what it is done in [6] for $P_{w,d}^{(K)}(m)$, we start by writing the expression of the contribution of the uplink noise at the output of the equalizer, namely $\mathbf{W}_u = \mathbf{W}_{u,\mathrm{even}} \otimes [1,0] + \mathbf{W}_{u,\mathrm{odd}} \otimes [0,1]$, where

$$\mathbf{W}_{u,*} = \sqrt{2A} \sum_{l=0}^{K-1} \sum_{s=1}^{L_d} \frac{h_d[s]}{M^l} \mathbf{\Lambda}_{H^{(0)}}^{-1} \mathbf{K}_l \mathbf{\Theta}_M^{s-1} \mathbf{\Phi}\mathbf{F}_M^H \times \left(\mathbf{N}_{u,*} \circledast (\mathbf{J}_M \mathbf{Q}^{(l)}(s))\right), \quad * \in \{\mathrm{even}, \mathrm{odd}\}.$$

The $M \times (N_s + \kappa)$ matrices $\mathbf{N}_{u,*}$ are filled with the elements of the relay noise vector $\mathbf{n}_u = [\mathbf{n}_{u,0}^T \mathbf{n}_{u,1}^T \dots \mathbf{n}_{u,2(N_s+\kappa)}^T]^T$ according to

$$\mathbf{N}_{u,\mathrm{even}} = \begin{bmatrix} \mathbf{n}_{u,0} & \mathbf{n}_{u,2} & \cdots & \mathbf{n}_{u,2(N_s+\kappa-1)} \\ \mathbf{n}_{u,1} & \mathbf{n}_{u,3} & \cdots & \mathbf{n}_{u,2(N_s+\kappa)-1} \end{bmatrix}$$

and

$$\mathbf{N}_{u,\mathrm{odd}} = \begin{bmatrix} \mathbf{n}_{u,1} & \mathbf{n}_{u,3} & \cdots & \mathbf{n}_{u,2(N_s+\kappa)-1} \\ \mathbf{n}_{u,2} & \mathbf{n}_{u,4} & \cdots & \mathbf{n}_{u,2(N_s+\kappa)} \end{bmatrix},$$

respectively. Now, denoting by $\mathbf{w}_{u,*}(r)$ the r-th column of $\mathbf{W}_{u,*}$, the uplink noise vector component corresponding to the r-th multicarrier symbol after destaggering can be written as $\boldsymbol{\omega}_r = \mathrm{Re}\{\mathbf{w}_{u,\mathrm{odd}}(r)\} + j\,\mathrm{Im}\{\mathbf{w}_{u,\mathrm{even}}(r+1)\}$. After some algebra, the covariance matrix of $\boldsymbol{\omega}_r$ can be shown to be

$$\mathbf{C}_u = A\sigma_u^2 \sum_{l,r=0}^{K-1} \sum_{s,t=1}^{L_d} \frac{1}{M^{l+r}} \begin{bmatrix} \mathrm{Re}\left\{h_d[s]\Lambda_{H^{(0)}}^{-1}\mathbf{K}_l\mathbf{\Theta}_M^{s-1}\right\} \\ \mathrm{Im}\left\{h_d[s]\Lambda_{H^{(0)}}^{-1}\mathbf{K}_l\mathbf{\Theta}_M^{s-1}\right\} \end{bmatrix}^T \times \begin{bmatrix} \mathbf{D}_{l,r}^{s,t} & -j\tilde{\mathbf{D}}_{l,r}^{s,t} \\ j\tilde{\mathbf{D}}_{l,r}^{s,t} & \mathbf{D}_{l,r}^{s,t} \end{bmatrix} \begin{bmatrix} \mathrm{Re}\left\{h_d[t]\Lambda_{H^{(0)}}^{-1}\mathbf{K}_r\mathbf{\Theta}_M^{t-1}\right\} \\ \mathrm{Im}\left\{h_d[t]\Lambda_{H^{(0)}}^{-1}\mathbf{K}_r\mathbf{\Theta}_M^{t-1}\right\} \end{bmatrix},$$

where

$$\mathbf{D}_{l,r}^{s,t} = \mathbf{\Phi}\mathbf{F}_M^H\Big[\mathrm{diag}\left\{\mathbf{U}^+\mathbf{r}_{l,r}^{s,t}\right\} + \mathrm{diag}\left\{\mathbf{U}^-\mathbf{s}_{l,r}^{s,t}\right\}(\mathbf{J}_2 \otimes \mathbf{I}_{M/2})\Big]\mathbf{F}_M\mathbf{\Phi}^*,$$

$$\tilde{\mathbf{D}}_{l,r}^{s,t} = \mathbf{\Phi}\mathbf{F}_M^H\Big[\mathrm{diag}\left\{\mathbf{U}^-\mathbf{r}_{l,r}^{s,t}\right\} + \mathrm{diag}\left\{\mathbf{U}^+\mathbf{s}_{l,r}^{s,t}\right\}(\mathbf{J}_2 \otimes \mathbf{I}_{M/2})\Big]\mathbf{F}_M\mathbf{\Phi}^*,$$

with

$$\mathbf{s}_{l,r}^{s,t} = \begin{bmatrix} \left\{\mathcal{S}\left(\tilde{q}_N^{(l)}(s), q_N^{(r)}(t)\right)\right\}_{1:M/2,\kappa} \\ \left\{\mathcal{S}\left(\tilde{q}_N^{(l)}(s), q_N^{(r)}(t)\right)\right\}_{M/2+1:M,\kappa+1} \end{bmatrix}.$$

The power of the uplink noise component at the m-th subcarrier, that is $P_{w,u}^{(K)}(m)$, is hence the m-th element of the diagonal of $\mathbf{C}_u$. ■

III. Numerical Results

To assess the results presented above, we consider a system where the relay is placed on the source–destination line of unitary length. We take 128 subcarriers separated by 15 kHz, so that the sampling frequency is 1.920 MHz. The chosen prototype pulse (at both the transmitter and the receiver side) is the one proposed by the PHYDYAS ICT project [7], with overlapping factor $\kappa = 4$, depicted in Fig. 1.

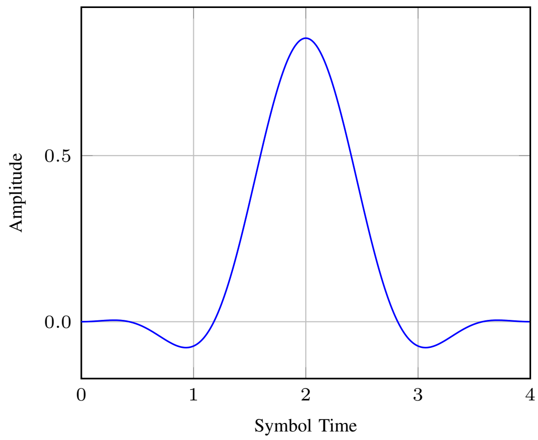

Fig. 1. Prototype pulse used in all simulations.

The uplink (source to relay) and downlink (relay to destination) channels are generated according to the Extended Vehicular A (EVA) model [8]. In order to have a fair comparison between the AF relay channel and the direct link, we proceed as follows: the direct channel is obtained by taking the convolution of the uplink and downlink channels of the relay after having normalized their path loss to 1. Moreover, the path losses of the uplink channel and of the downlink channel are given by $d^{-\alpha}$ and $(1-d)^{-\alpha}$, respectively, where $d \in (0,1)$ is the distance from the source to the relay and α is the path-loss exponent. Also, we assume that the additive white Gaussian noise on both channels has the same variance, namely $\sigma_u^2 = \sigma_d^2 = \sigma^2$.

Finally, note that we focus on full-duplex relays that can transmit and receive at the same time. For simplicity, we assume an ideal/perfect electromagnetic separation between the receiving and the transmitting RF chains at the relay, thus neglecting all self-interference issues. Denoting by P_s the total available power in the system, we fix $P_{tx} = P_r = P_s/2$. Note that relay transmitted power P_r is obtained by taking $A = P_r/(2\frac{P_{tx}}{M}\sum_{n=1}^{N} p_N^2[n]\sum_{l=1}^{L_u}|h_u[l]|^2 + \sigma_u^2)$. Conversely, we have $P_{tx} = P_s$ when the direct link with no relay is considered.

To start with, in Fig. 2 and Fig. 3, we compare the theoretical results of the previous section with empirical ones, obtained by averaging the measured SNDR of $N_s = 1000$ multicarrier 4-QAM symbols transmitted over the same channel. The SNR, defined as the ratio between the total power P_s and the noise variance σ^2, is set to 20 dB and 40 dB, respectively. First of all, in Fig. 3, we note that the difference between the empirical results and the theoretical ones increases as we increase the number of equalization stages K. This is due to the fact that the chosen pulse does not perfectly fulfill reconstruction constraints (and the assumptions on its derivatives required by [6]) and, thus, the expression (4) of the residual interference power is not exact anymore. This fact can only be noticed at high SNR (e.g., Fig. 3, 40 dB), where the residual interference after equalization is the most significant source of error. On the other hand, at lower and more practical SNR values (e.g., Fig. 2, 20 dB), the approximation is tighter, since the noise is the dominating impairment. As a final remark, note that at SNR=20 dB, there is a noticeable gain of almost 5 dB when going from $K = 1$ to $K = 2$ equalization stages, while adding a third stage brings almost no benefits.

Having verified that the empirical results fit to the theoretical ones, we now use the latter to compare the AF relay channel to the direct point-to-point channel. More specifically, for a relay placed half way from the source to destination (that is $d = 0.5$), we investigate the mean spectral efficiency over the M subcarriers, namely

$$I = \frac{1}{M}\sum_{m=1}^{M} \ln(1 + SNDR_{K,\mathrm{AF}}(m)) \tag{8}$$

where $SNDR_{K,\mathrm{AF}}(m)$ is given by (6). The curves in Fig. 4 and Fig. 5 are obtained averaging 500 different channel realizations. Apart from the spectral efficiency of the AF relay channel, the figures also report the results of the direct link and of two different flavors of DF relay. More specifically, the spectral efficiency of the direct link is computed as in (8) but using the SNDR expression for a point-to-point channel in (3). On the other hand, a DF relay splits the channel into two separate hops and each one of them can be seen as a point-to-point link. The end-to-end spectral efficiency is hence the minimum between the spectral efficiency of the two hops. We can consider two different encoding schemes: the first scheme (the DF-1 curve) encodes each subcarrier stream independently of the others and, then, the spectral efficiency is computed as $I_{\mathrm{DF}-1} = \frac{1}{M}\sum_{m=1}^{M}\ln\Big(1 + \min\Big\{SNDR_K^{(up)}(m), SNDR_K^{(down)}(m)\Big\}\Big)$. The second scheme (the DF-2 curve), instead, corresponds to the case where all the subcarriers streams are encoded jointly to exploit the diversity offered by the FBMC modulation. The resulting spectral efficiency is $I_{\mathrm{DF}-2} = \frac{1}{M}\min\Big\{\sum_{m=1}^{M}\ln\Big(1 + SNDR_K^{(up)}(m)\Big), \sum_{m=1}^{M}\ln\Big(1 + SNDR_K^{(down)}(m)\Big)\Big\}$. Note that, according to the idea that the relay should be a simple

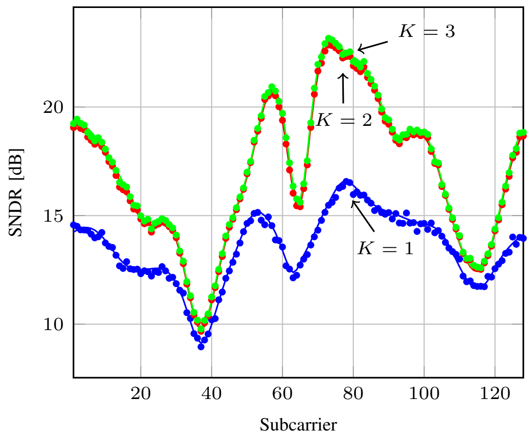

Fig. 2. Comparison of simulated (dots) and theoretical (lines) values of SNDR at $SNR = P_s/\sigma^2 = 20$ dB and for different numbers of equalization stages.

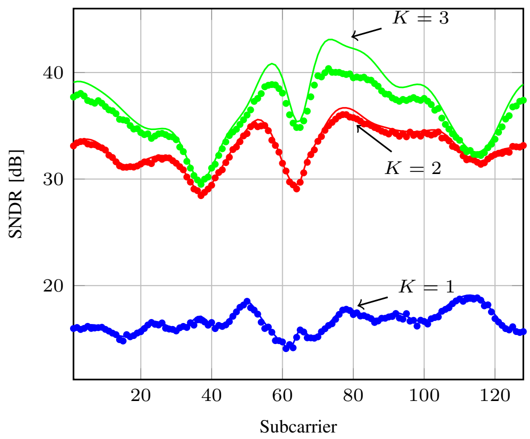

Fig. 3. Comparison of simulated (dots) and theoretical (lines) values of SNDR at $SNR = P_s/\sigma^2 = 40$ dB and for different numbers of equalization stages.

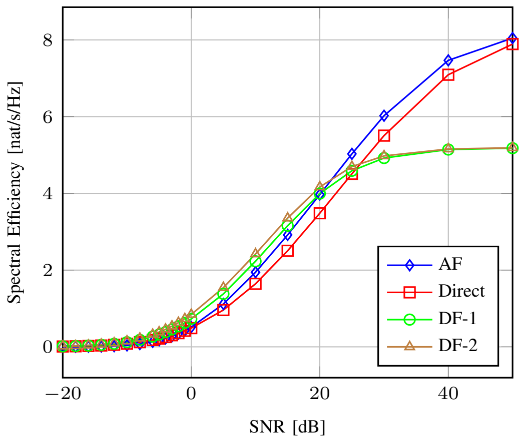

Fig. 4. Mean per-subcarrier spectral efficiency as function of the SNR for $\alpha = 2.5$ and averaged over 500 channel realizations.

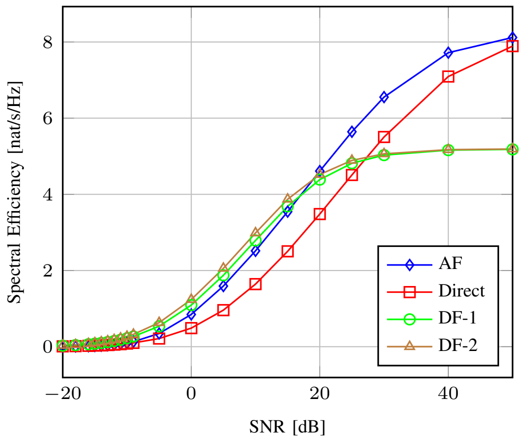

Fig. 5. Mean per-subcarrier spectral efficiency as function of the SNR for $\alpha = 3.5$ and averaged over 500 channel realizations.

device, the number of equalization stages at the DF relay has been fixed to one, as opposed to $K = 2$ for the equalizer at the destination.

Both Fig. 4 and Fig. 5 show that the AF relay improves the spectral efficiency of the link for a wide range of SNR values. Moreover, the gain over the direct link increases with the path-loss exponent. For example, for a spectral efficiency of 4 nat/s/Hz, the gain is around 2 dB for $\alpha = 2.5$ (Fig. 4) and around 5 dB for $\alpha = 3.5$ (Fig. 5). A higher gain for larger path-loss exponents was expected, since the channel quality of short links—as compared to a long one—is higher when the path-loss exponent takes large values.

From the two figures one can also realize that the spectral efficiency of both the AF relay channel and the direct link saturate at a common value around 8 nat/s/Hz as the SNR grows large. The reason for this is that the residual interference power $P_{e,\text{AF}}^{(K)}(m)$ in (4) does not depend on the SNR. Actually, the ratio $P_{tx}/P_{e,\text{AF}}^{(K)}(m)$ only depends on the shape (and not on the amplitude) of the channel. Then, as the noise power tends to zero, the SNDR tends to $P_{tx}/P_{e,\text{AF}}^{(K)}(m)$. In our simulations, this ratio takes the same value for both protocols, since we have built the direct link as a normalized version of the AF relay channel.

As for the DF relay, we see that its spectral efficiency saturates to a much lower value (just above 5 nat/s/Hz) at high SNR. One should recall that the number of equalization stages at the relay has been fixed to one, in order to contain complexity. This is indeed the bottleneck of the DF relay channel, as it can be readily guessed from Fig. 2 and Fig. 3. Conversely, for medium values of SNR, the per-subcarrier DF relay (DF-1) gains 1 dB over the AF relay as a result for not forwarding noise. By further increasing complexity, an extra decibel can be gained if all the subcarriers are jointly encoded (DF-2).

IV. Conclusions

In this paper we have considered a two-hop FBMC/OQAM link with an AF relay. For a nontrivial equalizer with K parallel stages, the quality of the signal at the m-th subcarrier has been characterized in terms of signal-to-noise-plus-distortion ratio, which takes into account the residual interference after equalization and the effect of the noise collected on both the source–relay channel and the relay–destination channel. The resulting theoretical expression of the SNDR fits with the numerical results.

In order to evaluate whether the relay improves the quality of the link, the AF scheme has been compared, in terms of spectral efficiency, to the direct source–destination link and to another relay solution employing decode and forward. In the considered scenario we have seen that relaying shows its highest gain for practical SNR values between 0 dB and 30 dB, especially in lossy environments with high path-loss exponents. On the other hand, further investigation is needed in the low-SNR regime, where there is little to no gain over the direct link. Intuitively, a possible explanation is that the equivalent channel seen by the data symbols depends on the relay transmitted power through the amplification factor A. Thus, at low SNR, the channel inversion realized by the equalizer is an undetermined operation.

References

[1] Project PPDR-TCenter FP7-SEC 313015. [Online]. Available: http://www.ppdr-tc.eu/

[2] Project EMPhAtiC FP7-ICT 318362. [Online]. Available: http://www.ict-emphatic.eu/

[3] Project SAN CP08-011. [Online]. Available: http://projects.celtic-initiative.org/SAN/

[4] Project ABSOLUTE FP7-ICT 318632. [Online]. Available: http://www.absolute-project.eu/

[5] J. N. Laneman, D. N. C. Tse, and G. W. Wornell, “Cooperative diversity in wireless networks: Efficient protocols and outage behavior,” *IEEE Trans. Inf. Theory*, vol. 50, no. 12, pp. 3062–3080, Dec. 2004.

[6] X. Mestre, M. Majoral, and S. Pfletschinger, “An asymptotic approach to parallel equalization of filter bank based multicarrier signals,” *IEEE Trans. Signal Process.*, vol. 61, no. 14, pp. 3592–3606, Jul. 2013.

[7] A. Viholainen *et al.*, “Prototype filter and structure optimization,” Project PHYDYAS ICT-211887, Deliverable D5.1, Jan. 2009.

[8] 3rd Generation Partnership Project, “LTE; evolved universal terrestrial radio access (e-UTRA); base station (BS) radio transmission and reception,” ETSI, Tech. Spec. TS36.104 v11.4.0 release 11, 2013.